Mon. Not. R. Astron. Soc. **000**, 1–?? (2010) Printed 9 October 2015 (MN LATEX style file v2.2)

Strongly Coupled Dark Energy Cosmologies: preserving ΛCDM success and easing low scale problems II - Cosmological simulations

Andrea V. Macciò[1⋆], Roberto Mainini[2], Camilla Penzo[1], Silvio A. Bonometto[3]
[1]*Max-Planck-Institut für Astronomie, Königstuhl 17, 69117 Heidelberg, Germany*
[2]*Milano–Bicocca University, Physics Department G. Occhialini, Piazza della Scienza 3, 20126 Milano-Bicocca*
[3]*Trieste University, Physics Department, Astronomy Unit, Via Tiepolo 11, 34143 Trieste (Italy) & I.N.A.F., Osservatorio Astronomico di Trieste*

Accepted XXXX . Received XXXX; in original form XXXX

ABSTRACT

In this second paper we present the first Nbody cosmological simulations of strongly coupled Dark Energy models (SCDEW), a class of models that alleviates theoretical issues related to the nature of dark energy. SCDEW models assume a strong coupling between Dark Energy (DE) and an ancillary Cold Dark Matter (CDM) component together with the presence of an uncoupled Warm Dark Matter component. The strong coupling between CDM and DE allows us to preserve small scale fluctuations even if the warm particle is quite light ($\approx$ 100 eV). Our large scale simulations show that, for $10^{11} < M/M_{\odot} < 10^{14}$, SCDEW haloes exhibit a number density and distribution similar to a standard Lambda Cold Dark Matter (ΛCDM) model, even though they have lower concentration parameters. High resolution simulation of a galactic halo ($M \sim 10^{12}\mathrm{M}_{\odot}$) shows $\sim 60\%$ less substructures than its $\Lambda\mathrm{CDM}$ counterpart, but the same cuspy density profile. On the scale of galactic satellites ($M \sim 10^{9}\mathrm{M}_{\odot}$) SCDEW haloes dramatically differ from $\Lambda\mathrm{CDM}$. Due to the high thermal velocities of the WDM component they are almost devoid of any substructures and present strongly cored dark matter density profiles. These density cores extend for several hundreds of parsecs, in very good agreement with Milky Way satellites observations. Strongly coupled models, thanks to their ability to match observations on both large and small scales might represent a valid alternative to a simple $\Lambda\mathrm{CDM}$ model.

Key words:
cosmology: dark matter galaxies: evolution - formation methods:N-body simulation

1 INTRODUCTION

A large variety of data on both small and large scales points to the existence of two dark components in our Universe: dark matter, which dominates the gravitational budget of collapsed objects like galaxies and clusters, and dark energy, which regulates the expansion of the Universe at later times (Tegmark et al. 2006, Planck collaboration 2014). While there is a general agreement on the presence of these two components, their nature is still very unclear and several possibilities have been put forward in the last years.

The most common model for Dark Matter (DM) and Dark Energy (DE) is the Lambda Cold Dark Matter ($\Lambda\mathrm{CDM}$). In this model DE behaves like a cosmological constant, being often interpreted as vacuum energy, and is therefore constant in space and time. Furthermore, DM particle velocities are assumed to be negligible, as though they decoupled quite early being already non–relativistic.

The $\Lambda\mathrm{CDM}$ model is quite successful in reproducing data on large and intermediate scales (e.g. Springel et al. 2005). On the other hand it still raises several questions like the fine tuning problem, as the DE energy density is $\sim (10^{-30}m_p)^4$ (m_p : Planck mass), and the coincidence or *"Why now?"* problem: why DE, negligible during all cosmic history, became significant just now and late enough to allow non–linear structures to develop.

In the attempt to alleviate these problems, the option of DE being a self–interacting scalar field with a tracker potential was suggested (e.g., Ellis et al, Wetterich 1988, Ratra & Peebles 1988, Brax & Martin 1999, 2000, see Ratra & Peebles 2003 for a review). Furthermore the possibility of a coupling between DM and DE was deepened by several authors (e.g. Wetterich 1995, Amendola 2000

⋆ E-mail: maccio@mpia.de

Amendola & Tocchini–Valentini 2001, see Amendola et al. 2013 and references therein for a comprehensive review).

While tracker potentials are devoid of finely tuned scales, the coupling allows for a non-negligible fraction of DE at early times (e.g. Amendola 2000). As expected, DM–DE coupling modifies the equation of motion of a test particle in an expanding universe with respect to the pure Newtonian case (Macciò et al. 2004).

In the past years several works studied the effect of a DM-DE coupling on structure formation (e.g. Macciò et al. 2004, Calderа-Cabral et al. 2009, Baldi et al. 2010, Li & Barrow 2011, Baldi 2012). After Planck data release, Xia (2014) outlined that the tension between CMB and Hubble telescope H_0 estimates was eliminated by the coupling option, finding a coupling constant $\beta = 0.078 \pm 0.022$. Other observables, however, are not significantly modified by such coupling and this makes it hard to disentangle coupled dark energy models from a more simple ΛCDM one (e.g. Baldi et al. 2012, Pace et al. 2015).

The ΛCDM model also faces some tension with data on the scales of low mass galaxies where the central cuspy dark matter distribution predicted by CDM (e.g Navarro, Frenk & White 1997) seems to be a very poor match of the observed central cored dark matter distribution in dwarf galaxies (e.g. Moore 1994, de Blok et al. 2001, Kuzio de Naray et al. 2006, Oh et al. 2011, Salucci et al. 2012).

In the last years, there has been a mounting evidence that including the effect of a dissipational baryonic component, strongly modifies the central DM distribution (Governato et al. 2010, Macciò et al. 2012a) reconciling observations and simulations on dwarf galaxy scales (Di Cintio et al. 2014a).

On the other hand these simulations have also shown that baryons are effective in altering the DM density profile only up to a certain mass scale (Governato et al. 2012, Di Cintio et al. 2014b, Arraki et al. 2014, Oñorbe et al. 2015) and that very low mass galaxies are expected to retain a cuspy profile.

Unfortunately this is in contrast with recent observations of the DM distribution in the MW satellites, which seem to suggest the presence of cored profiles even at these very low mass scales, where the effect of baryons should be minimal. The presence of such cores might indicate that DM is warm (e.g. Dalcanton & Hogan 2001, Colin et al. 2008). Several works have dealt with the effect of Warm Dark Matter (WDM) on halo structure (Bode et al. 2001, Avila-Reese et al. 2001, Knebe et al. 2002, Tikhonov et al. 2009, Schneider et al. 2012). Constraints on the mass of a possible WDM candidate can be obtained from the analysis of the matter power spectrum from the Lyman–α forest (Seljak et al. 2006, Viel et al. 2005,2008, Boyarsky et al. 2009), current measurements suggest the WDM mass (for a pure thermal candidate) to be around (or above) 3.5 keV (Viel et al. 2013, Polisensky & Ricotti 2014).

A WDM particle of 3–4 keV, however, yields no improvement with respect to CDM on small scales (Schneider et al. 2014). The situation is particularly hopeless for halo density profiles, which require a WDM particle of ~ 100 eV in order to create appreciable central cores as the ones observed in the Milky Way satellites (Macciò et al. 2012b, Shao et al. 2013).

In the light of these considerations it is worth to explore alternatives to ΛCDM , aiming to a model which can deal, at the same time, with both theoretical and observational issues.

In two recent papers (Bonometto et al. 2012, Bonometto & Mainini 2014) a new model was indeed proposed, which combines DM-DE coupling and Warm Dark Matter trying to overcome the problems of ΛCDM , both on the theoretical and observational side. Observational DM, in this model, is warm and light. An auxiliary CDM component, coupled to DE, is however added, which never exceeds some permils of the total density, but naturally exerts a number of key effects though cosmic history.

In the companion paper (Bonometto, Mainini, Macciò 2015, Paper I hereafter) we addressed the linear behavior of such models also including a new option, that CDM–DE coupling fades at low z. In these models WDM is made of extremely low mass particles, down to few tens of eV, which might, in turn, have significant effects on the central DM distribution in collapsed objects.

In this second paper, we aim to present the first Nbody simulations of strongly coupled warm+cold models (SCDEW hereafter). Our goal is to study these models in the highly non linear regime probed by structure formation, both on large ($\sim$Mpc) and small ($\sim$100 pc) scales.

The paper is organized as follows: we will first summarize the main features of our novel cosmological model in section (2), we will then introduce our numerical codes to generate initial conditions and evolve the simulations (3), we will then present results for large scales simulations and for zoomed simulations of Milky Way-like objects and dwarf galaxies (4), we will then conclude with a discussion of our results and possible future developments (5).

2 THEORETICAL MODEL

In this Section we briefly review the main features of SCDEW cosmologies, more extensively discussed in the previous associated paper. Besides of baryonic and radiative components (γ's & ν's), these models assume an ordinary uncoupled light WDM component, while DE is coupled to an ancillary CDM component which, actually, never plays the role that DM has in ΛCDM or similar models.

The starting point of SCDEW cosmologies is the finding that, during radiative expansion, an attractor solution exists, for coupled CDM and a scalar field components, keeping them a constant fraction of the cosmic density in primeval radiative eras. In the absence of coupling, these components would dilute $\propto a^{-3}$ and $\propto a^{-6}$ respectively. The time evolution of the different density parameters as a function of the expansion factor a in our SCDEW model is presented in figure 1.

As shown in the Figure, the coupling, by allowing energy to flow from CDM to the field, puts CDM and DE on an attractor solution where both shall dilute $\propto a^{-4}$, as radiative components do. For a coupling constant β, the fair constant primeval density parameters of the two components, along the attractor, are $1/2\beta^2$ and $1/4\beta^2$, respectively. Values $\beta \sim 10$ are favored, so that the early contribution of CDM and field keeps steadily around or below $\approx 0.2\,\%$. While causing no harm to BBN or CMB data, this contribution therefore keeps non–negligible, possibly dating since the end of inflation.

When this stationary solution is broken by WDM derelativisation, the Universe naturally evolves towards the observed features. In particular, the field turns into the observed DE component.

Accordingly, at variance from ΛCDM models, in SCDEW models DE has always been a small but non–negligible component, which eases fine tuning while the coincidence problem is also attenuated, for a wide set of parameter choices, including those needed to obtain a reasonable fit to large scale data. The option of the field Φ playing both the role of inflaton and DE is also not excluded.

Coupled CDM however plays another key role. In the non–relativistic regime, as already known (Amendola 2000), its coupling to DE causes a strengthening of its self-gravity. This triggers

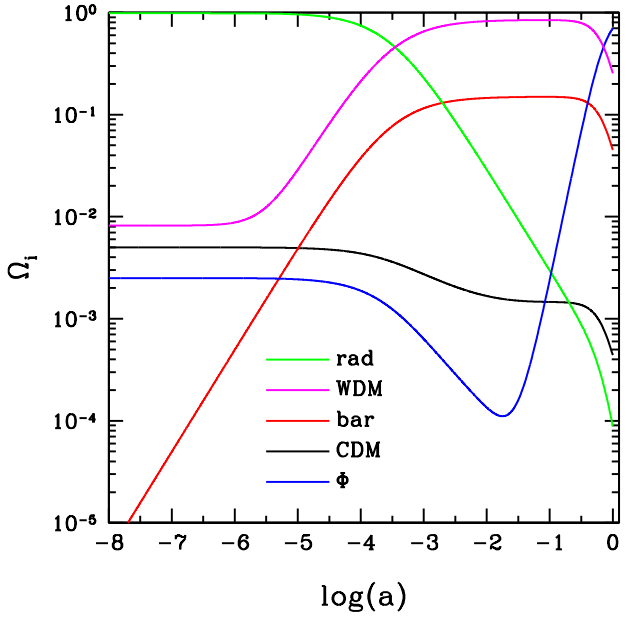

Figure 1. Time evolution of the density parameters (Ω_i) of radiation, Dark Energy (Φ), Cold Dark Matter, Warm Dark Matter and baryons in the SCDEW model.

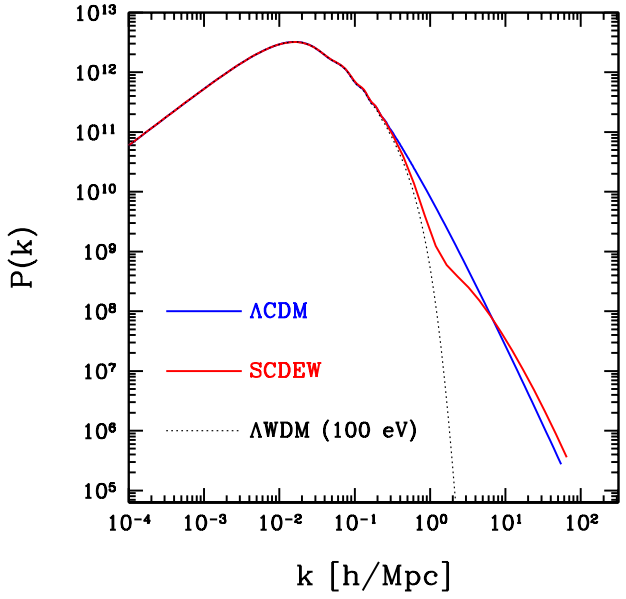

Figure 2. Linear power spectrum at z=0 for the ΛCDM model (blue) and the SCDEW model (red). The black thin line shows, for comparison, the power spectrum of a Lambda Warm Dark Matter model (LWDM) with a particle mass of 90 eV.

a mechanism allowing its fluctuations to restart WDM fluctuations, also on scales where they had formerly been erased by free streaming, as soon as WDM derelativizes. This revitalization of WDM fluctuations on scales below the free streaming one allows us to have very "hot" WDM, of the order of 100 eV.

At more recent times ($z <\sim 50$), besides of keeping a density parameter $< 10^{-1}$–10^{-2} of baryons, CDM could dynamically decouple from baryon and WDM fluctuations.

This decoupling might arise naturally, however in our current parameterization we have imposed an *ad-hoc* decoupling at small redshifts, which causes no substantial change in the expected fluctuation spectra. Of course a full consistent model should provide a mechanism for the fading of the coupling at low redshift, which, for example, can be a conseguence of the dynamics of the scalar field. We refer the reader to Paper I (especially appendix A) for a thourough discussion of this issue while here we rather prefer to use a more phenomelogical approach.

For the sake of definiteness, therefore, the linear spectra used to start the simulations in this work are those obtainable by setting a decoupling parameter $d = 4$ (see Paper I), yielding a full CDM–DE decoupling at $z \simeq 50$, where simulations are started.

3 NUMERICAL SIMULATIONS

Numerical simulations have been performed with the Nbody code PKDGRAV (Stadel et al. 2001), while the initial conditions have been created with the GRAFIC2 code (Bertchinger 2001), which we have recently modified to allow a larger spectrum of cosmological models, as described in Penzo et al. (2014). The transfer function for the power spectrum have been produced with a modified version of CMBFAST that allows for an explicit coupling between the cold dark matter and the dark energy components (Bonometto & Mainini 2014).

The redshift–zero power spectrum for our specific SCDEW model is shown in figure 2. Despite the presence of a very warm component with a mass of 90 eV, the power spectrum does not differ much from the expectation of a ΛCDM model with the same cosmological parameters. For the sake of comparison, in the same figure we also show the power spectrum of a pure WDM model for the same warm particle mass. As expected, it exhibit a dramatic reduction of the power on small scales.

As is evident from Figure 1, at the initial redshift of our simulations ($z \approx 50$), the CDM contribution to the gravitational potential is quite small. When combined with our assumption of a vanishing coupling at late times (see Paper I), this allows us to use the standard equations of motions for the Warm Dark Matter components and to neglect the presence of a Cold component in the simulation. On the other hand the initial power spectrum and the evolution of the background do account for the presence of all components, i.e., essentially, the effects of a fair time dependence of Dark Energy.

Finally, in agreement with previous works on WDM (Colin et al. 2008, Macciò et al. 2012b, Shao et al. 2013), WDM particles were added the thermal velocity

$$\frac{v_0(z)}{1+z} = .012 \left(\frac{\Omega_{\rm w}}{0.3}\right)^{\frac{1}{3}} \left(\frac{h}{0.65}\right)^{\frac{2}{3}} \left(\frac{1.5}{g_{\rm w}}\right)^{\frac{1}{3}} \left(\frac{\rm keV}{m_{\rm w}}\right)^{\frac{4}{3}} {\rm km\,s^{-1}} \quad (1)$$

in agreement with Bode et al. (2001); here z is the redshift, h is the Hubble parameter in unit of 100 (km/s)Mpc^{-1}, $\Omega_{\rm w}$, $m_{\rm w}$ and $g_{\rm w}$ are the density parameter, the mass and the number of spin states of WDM respectively. Their distribution function reads then $(e^{p_{\rm w}/T_{\rm w}}+1)^{-1}$ ($p_{\rm w}$ and $T_{\rm w}$ being the momentum and temperature of WDM), until gravitational clustering begins (Bode et al. 2001).

Table 1. Cosmological parameters for the ΛCDM and SCDEW models. Here Ω_Φ, Ω_c, $\Omega_{\rm w}$ and Ω_b are the density parameters of DE,CDM, WDM and baryons. All models share the same values for the Hubble parameter ($h = 0.685$), the spectral index ($n_s = 0.968$) and the power spectrum normalization ($\sigma_8 = 0.833$).

Label	Ω_Φ	Ω_c	$\Omega_{\rm w}$	Ω_b	$m_{\rm w}$ [eV]
SCDEW	0.704	0.001	0.250	0.045	90
ΛCDM	0.704	0.251	–	0.045	–

Table 2. High resolution simulations properties.

Halo	Model	$M_{\rm vir}$ $[h^{-1}\,{\rm M}_\odot]$	$N_{\rm vir}$	Softening $[h^{-1}{\rm kpc}\,]$
MW1	SCDEW	8.51×10^{11}	1,573,013	0.4
MW1	ΛCDM	9.11×10^{11}	1,685,767	0.4
D1	SCDEW	8.92×10^{9}	1,501,683	0.1
D2	SCDEW	1.31×10^{10}	2,205,387	0.1
D1L	ΛCDM	7.51×10^{9}	1,264,309	0.1

3.1 Large Box simulations

We run two kinds of simulations, the first in a set of fairly large cosmological boxes with the same resolution across the whole box. We have three different volumes with $L = 20,\ 40,\ 90h^{-1}{\rm Mpc}$ aside, each of them containing 300^3 dark matter particles. For each box we run two simulations, one with our SCDEW model, and a reference one done in standard ΛCDM for the same set of cosmological parameters (see table 1 for a complete list). We have used same values for the Hubble constant ($h = 0.685$), the spectral index ($n_s = 0.968$) and the power spectrum normalization ($\sigma_8 = 0.833$) in all models.

In all simulations, dark matter haloes are identified using a spherical overdensity (SO) algorithm as described in Dutton & Macciò (2014). For our ΛCDM cosmology the virial density at redshift zero is $\Delta(0) \simeq 95.0$ based on the fitting function of Mainini et al. (2003); we have used the same value for the SCDEW model as well.

For each SO halo in our sample we evaluated the concentration parameter following the procedure outlined in Macciò et al. (2008). Briefly, we first determine the halo density profile, by using the most bound particle as the location of the halo center. We then compute the density (ρ_i) in 50 equally spaced (in log) spherical shells. The minimum radius is the maximum between 1% of the virial radius, $R_{\rm vir}$, or 3 times the softening length and the maximum radius is $1.2R_{\rm vir}$. Errors on the density are estimated from the Poisson noise due to the finite number of particles in each mass shell. We fit these density profiles with the NFW expression (Navarro et al. 1997):

$$\rho_{\rm NFW}(r) = \frac{\delta_c \rho_{\rm cr}}{(r/r_s)(1+r/r_s)^2}; \qquad (2)$$

here r_s is the scale radius of the halo, δ_c is normalization parameter, and ρ_{cr} is the critical density of the Universe. Their values, and associated uncertainties, are obtained via a χ^2 minimization procedure using the Levenberg & Marquart method. We define the r.m.s. of the fit as

$$\rho_{\rm rms} = \sqrt{\frac{1}{N}\sum_i^N (\ln\rho_i - \ln\rho_{\rm m})^2}\,, \qquad (3)$$

$\rho_{\rm m}$ being the fitted NFW density distribution. Finally, following Macciò et al. (2007), we only selected relaxed haloes by requiring $\rho_{\rm rms} < 0.5$ and $x_{\rm off} < 0.07$. Here $\rho_{\rm rms}$ is the r.m.s. of the NFW fit to the density profile and $x_{\rm off}$ is the offset between the most bound particle and the center of mass, in units of the virial radius $R_{\rm vir}$.

3.2 High resolution zoomed simulations

We then selected a few haloes to be re-run at much higher resolution, so allowing a more detailed study of the effect of our SCDEW models on the inner structure of haloes (e.g. density profiles) and on their satellite population.

One halo comes from the 90 $h^{-1}{\rm Mpc}$ box and has a mass similar to our own Milky-Way ($\approx 10^{12}h^{-1}\,{\rm M}_\odot$). We will refer to it as MW1. This halo was run with a mass resolution increase of 4096, reaching a mass per particle of $5.41\times10^5 h^{-1}\,{\rm M}_\odot$ and a softening of 0.4 $h^{-1}{\rm kpc}$. For this halo we performed three different runs, a ΛCDM one, two SCDEW, either with thermal velocities or without them. In order to identify bound subhaloes we used the AHF[1] halo finder (Knollmann & Knebe 2009).

Two further haloes (D1 and D2) have a much lower mass, similar to dwarf galaxies ($\approx\ 5\times10^9 h^{-1}\,{\rm M}_\odot$), and have been selected from the 20 $h^{-1}{\rm Mpc}$ box. They were also zoomed in by a factor of 4096, obtaining in this case a mass per particle of $5.94\times10^3 h^{-1}\,{\rm M}_\odot$ and a softening of 0.1 $h^{-1}{\rm kpc}$.

Unfortunately, no ΛCDM counterpart of these haloes could be run. As a matter of fact, on such small scales there are a lot of modifications to the tidal gravitation field when moving from ΛCDM to SCDEW, which alter the evolution pattern of the same initial Lagrangian region. In order to have a ΛCDM analogous of our dwarf SCDEW galaxies, we then turned to the 20 $h^{-1}{\rm Mpc}$ box in ΛCDM and selected there a halo with mass and environment similar to the halo D2. We run it at high resolution, and will call it D1L. All the parameters of high resolution halos are summarized in table 2.

4 RESULTS

We will start by presenting the analysis of large box simulations. Figure 3 shows the halo mass function in the two different models (obtained by combining all three different boxes of sizes 20, 40, 90 $h^{-1}{\rm Mpc}$). As expected from the Power Spectrum behavior (see figure 2), the two mass functions agree at high masses (large scales), while exhibiting some discrepancy as the halo mass decreases. At intermediate masses the ΛCDM model (blue line) produces more haloes with respect to the SCDEW one, while at the lowest masses probed by our simulations ($M \approx 10^{10}h^{-1}\,{\rm M}_\odot$) there is an excess of haloes in the SCDEW model. Differences are small anywhere, never exceeding a factor of two.

The concentration–mass plot shown in figure 4 exhibits more significant differences between the two models. This is expected, since the concentration parameter is more sensitive than the halo mass function to changes in the cosmological background (Macciò et al. 2008). While SCDEW shows concentrations similar to ΛCDM at the highest and lowest masses we probe, SCDEW exhibits significantly lower concentrations at intermediate masses:

[1] The Amiga Halo finder (AHF) can be freely downloaded from http://www.popia.ft.uam.es/AMIGA

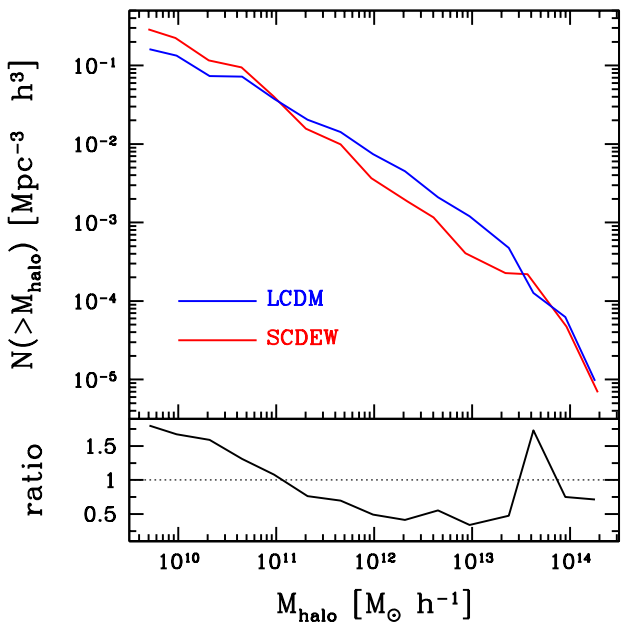

Figure 3. Halo Mass function at redshift zero: ΛCDM is shown in red, while SCDEW is shown in blue. The lower panel shows the ratio between the SCDEW and the ΛCDM mass functions.

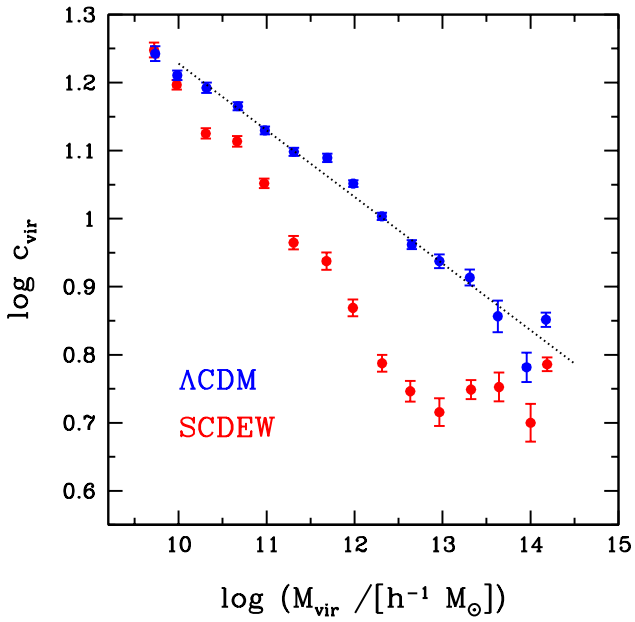

Figure 4. The concentration mass relation at $z = 0$. The blue points represent ΛCDM , while the red ones show SCDEW. The black dotted line shows a simple linear fit (in log-log space) to the ΛCDM results.

$5 \times 10^{10} - 5 \times 10^{13}\ h^{-1}\,\mathrm{M}_\odot$. These lower concentrations are due to lack of power on those scales, in the SCDEW model; haloes then form at a lower redshift, so determining lower concentrations (e.g. Wechsler et al. 2002).

As already noted in the Introduction, observations of low surface brightness galaxies and dwarf galaxies do suggest lower concentrations with respect to the predictions of a standard ΛCDM model (e.g. de Blok et al. 2001; van den Bosch & Swaters 2001; de Blok & Bosma 2002; Swaters et al. 2003; Dutton et al. 2005; Gentile et al. 2005; Simon et al. 2005) and hence they favor SCDEW.

4.1 Structure of Milky Way-like haloes in SCDEW

We will now study in more details the dark matter distribution and the satellites population in our two Milky Way-like high resolution dark matter haloes.

Figure 5 shows a logarithmic density map of the three versions of the MW1 halo: ΛCDM (left), SCDEW without initial thermal velocities (center) and SCDEW with thermal velocities (left). Even at naked eye, we notice a clear difference among the abundances of subhaloes in the three different cases.

These differences are quantified in figure 6 where we show the subhalo mass function for the above three simulations. The lower number of satellites in SCDEW with respect to ΛCDM is due to the combination of two effects: (i) There is less power on the MW scale; this delays the formation of the halo and lowers the environment density at the formation time; in turn, this reduces the subhaloes fraction (e.g. Maulbetsch et al. 2007). (ii) Furthermore, thermal velocities are high (WDM particles are 90 eV !) and this also suppresses the formation of low mass structures.

A comparison of the three lines in figure 6 clearly shows that on the scale of the Milky Way, the former effect is more important, while thermal velocities only affect the tail of the subhalo mass function at masses $M < 10^8 h^{-1}\,\mathrm{M}_\odot$.

The subhalo mass function in the SCDEW model is quite different from a pure Warm Dark Matter model, with the same WDM particle mass $m_\nu = 90eV$. In fact, in the latter case, the formation of *all* substructures is suppressed, since the free streaming mass for such a model is of the order of few $10^{14} h^{-1}\,\mathrm{M}_\odot$ (Zentner & Bullock 2003). On the contrary, in the SCDEW model, thanks to the coupling between CDM and DE, there are still enough substructures to host the formation of dwarf galaxies and, hence, not to violate constraints on the luminosity function of MW satellites (e.g. Macciò & Fontanot 2010).

Figure 7 shows the radial density profile for our three realizations of the MW1 halo. The ΛCDM profile (blue) is slightly higher in normalization w.r.t SCDEW, while sharing a similar slope; the virial concentration parameters are 10.4 for ΛCDM and 7.1 for SCDEW; the difference is mainly due to the slightly larger virial radius in the ΛCDM run. The difference between the SCDEW runs with and without velocities is almost negligible. This is not surprising given the halo mass and our choice of WDM mass (90 eV), we expect an effect on scales of few hundreds pc (e.g. Macciò et al. 2012), well below the resolution of our simulation. As we will see later, the situation is quite different for dwarf galaxies.

4.2 Structure of dwarf haloes in SCDEW

In order to investigate the effects of SCDEW on small spatial and mass scales we performed zoomed simulations of isolated dwarf haloes with masses of $M_{\mathrm{D1}} = 8.92 \times 10^9 h^{-1}\,\mathrm{M}_\odot$ and $M_{\mathrm{D2}} = 1.31 \times 10^{10} h^{-1}\,\mathrm{M}_\odot$. As already mentioned, due to the large differences in the tidal field between SCDEW and ΛCDM for such small scales, neither D1 nor D2 could be run in ΛCDM. We rather selected a different halo with a similar mass $M_{\mathrm{D1L}} = 7.51 \times 10^9 h^{-1}\,\mathrm{M}_\odot$ from the ΛCDM simulation, and run it at the same resolution; we dubbed it D1L.

Figure 8 shows the density map of the D1 halo with and with-

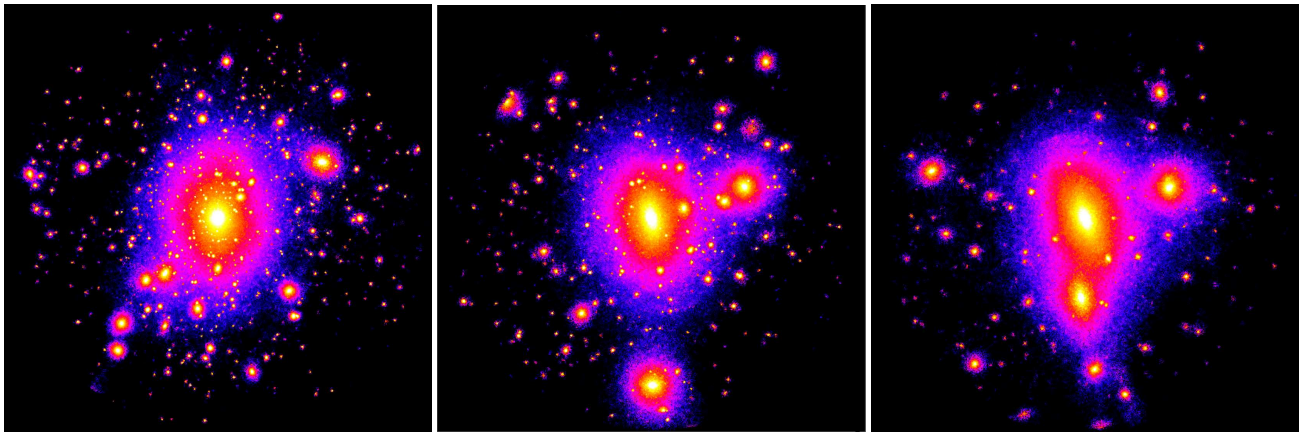

Figure 5. Logarithmic density map of the MW1 halo in the different models, each panel is 400 h^{-1}kpc across, encompassing the halo virial radius. Left ΛCDM , center SCDEW without thermal velocities, right SCDEW with thermal velocities.

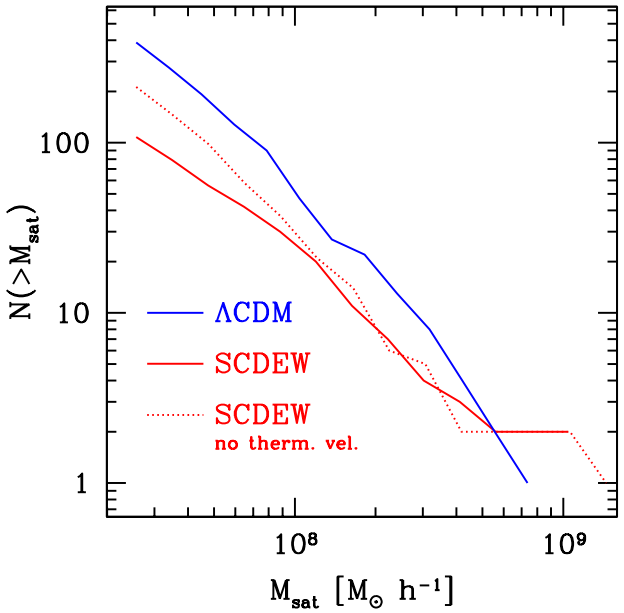

Figure 6. Subhalo integral mass function for the MW1 halo. ΛCDM is shown in blue, while the solid and dotted lines represent SCDEW with and without thermal velocities respectively.

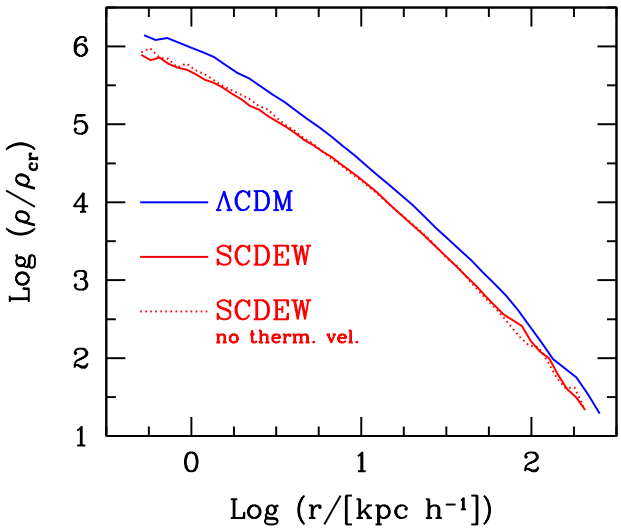

Figure 7. Density profile for the MW1 halo. ΛCDM is shown in blue, while the solid and dotted lines represent SCDEW with and without thermal velocities respectively.

out thermal velocities. At variance from what happened on the MW scale, in the SCDEW run with thermal velocities all subhaloes have disappeared, and only the central halo has survived. This sets an effective free streaming mass $\sim 10^7 h^{-1}$ M$_\odot$ for our model, equivalent to a warm dark matter (thermal) candidate of a few keV.

The most interesting effect of the presence of a warm component can be seen on the density profile of our dwarf galaxies. Figure 9 shows the density profile of the D1 (red) and the D1L (blue) haloes. The D1L profile exhibits the usual NFW–like shape with a cuspy central slope; the SCDEW profile *without* thermal velocities shows a NFW like behavior as well, with a cusp in the center, even if at a lower normalization.

The SCDEW halo *with* thermal velocities, instead, shows a very clear *cored* profile. The size of the core is of the order of several hundreds of pc, in agreement with theoretical expectations based on the conservation of phase space density (Macciò et al. 2012, Shao et al. 2013). Halo D2 exhibits a similar behavior, as shown in figure 10. The central slope of the profile is $\alpha = -0.25$, substantially shallower than the NFW prediction ($\alpha = -1$), even though the core is less pronounced. In this plot the blue line represents the theoretical expectation for an NFW profile in ΛCDM , assuming an average concentration for the halo D2 mass.

The flattening of the DM profile and the creation of a core on such small mass scales is one of the successes of the SCDEW model. Attempts of measuring the density profile of DM in the milky Way satellites suggests the presence of central cores (Walker & Peñarrubia 2011, Amorisco & Evans 2012, Amorisco et al. 2013) even though there is still some debate on whether cores are really needed to reproduce the kinematics of these satellites (Strigari

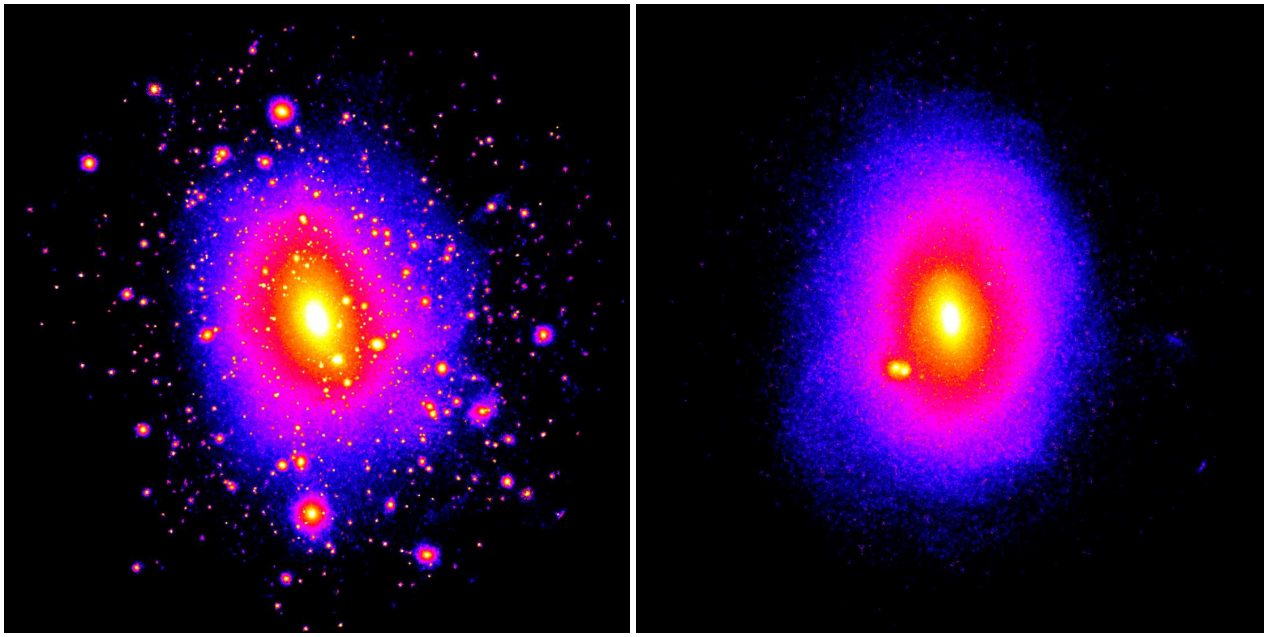

Figure 8. Density map, in logarithmic scale for the halo D1, each panel is 80 $h^{-1}\mathrm{kpc}$ across, encompassing the halo virial radius. Left SCDEW with out thermal velocities, right SCDEW with thermal velocities

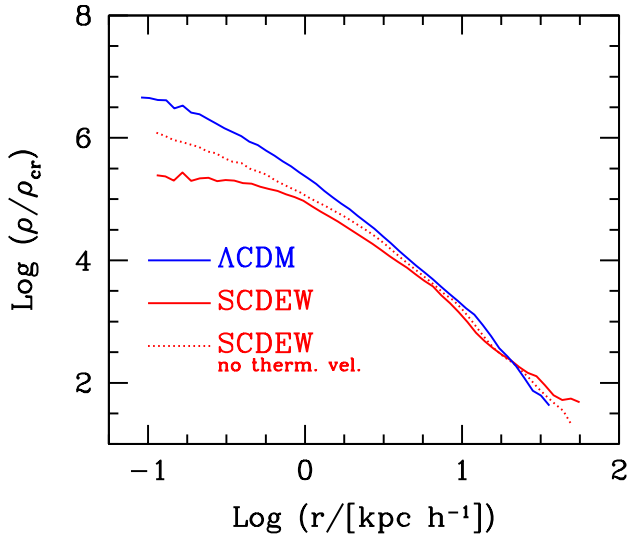

Figure 9. Density profile for the dwarf galaxy halo D1L (blue) and the D1 with velocities (solid red) and without them (dotted red).

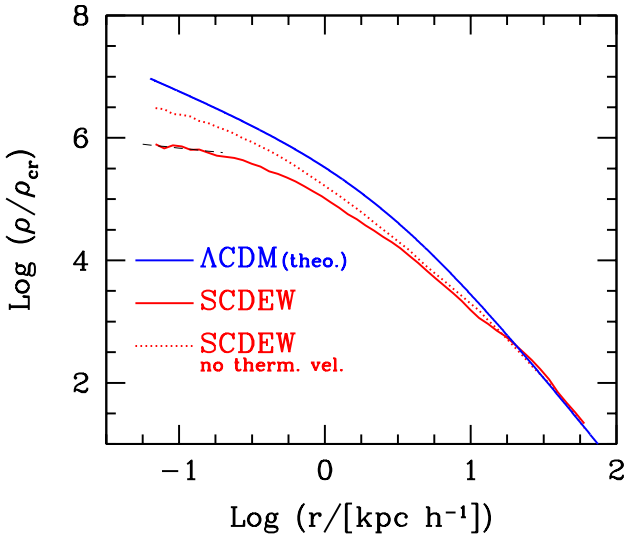

Figure 10. Density profile for the dwarf galaxy halo D2. SCDEW is shown as solid red, while SCDEW without velocities is shown by the dotted red line. The blue line is the $\Lambda\mathrm{CDM}$ theoretical expectation, for an NFW profile at this halo mass with an average concentration from figure 4.

et al. 2014). If cores are indeed present in such small objects, it is quite unlikely that their creation can be ascribed to baryonic effects (Garrison Kilmer et al. 2013), since the capability of baryons to modify the DM density profile is linked to the stellar/DM ratio, which is extremely low in these objects (Di Cintio et al. 14a).

Any cosmological model able to create cores at this mass scales will definitely ease the tension with the observations and hence should be preferred to a simple $\Lambda\mathrm{CDM}$ model.

5 CONCLUSIONS

The $\Lambda\mathrm{CDM}$ model (based on DE with state parameter $w \equiv -1$ and cold dark matter) is very successful in explaining the evolution of our Universe and its redshift zero structure (e.g. Tegmark et al. 2007).

Despite its success, this model faces problem on the theoret-

ical side, due to its inability to explain the very low value of DE density which, in turn, allows dark matter and dark energy densities to be quite similar at the present day. Furthermore, such low value allowed DE to become relevant late enough, so to allow primeval fluctuations to turn into non–linear structures up to quite large scales.

The ΛCDM scenario is also challenged by the possible presence of cores in the observed dark matter distribution of Milky Way satellites (e.g. Walker & Peñarrubia) since on such scales is very hard to invoke baryonic effects to reconcile observations and collisionless simulation predictions (Di Cintio et al. 2014a).

It is then worth to explore alternatives to the simple ΛCDM model, possibly trying to find a model that can deal, at the same time, with both theoretical and observational issues.

In this paper we presented a detailed non linear analysis of strongly coupled cold+warm cosmologies (SCDEW), while the linear theory and the basic features of these models have been presented in the companion paper (Bonometto, Mainini & Macciò 2015, Paper I).

Thanks to the coupling between Dark Energy and Cold Dark Matter, these models are able to ease the fine tuning and, possibly, the coincidence problem depending on the model parameters, problems that plage a simple ΛCDM scenario. A very important feature of SCDEW is that the (uncoupled) warm dark matter component can be chosen with very low particle mass, as low as ~ 100 eV, since the strongly coupled CDM is able to regenerate fluctuations in the WDM component after its derelativisation (see Paper I). As a consequence, the power spectrum of the SCDEW cosmology is very similar to the one of standard ΛCDM, and hence in very good agreement with observations.

We have run and analyzed several Nbody simulations performed in the SCDEW scenario and compared them with analogous simulations in the ΛCDM model. On large scales, SCDEW is quite similar to ΛCDM in halo distribution and number density; this implies that SCDEW shares the same success of ΛCDM on these scales. On the other hand, the distribution of mass in collapsed objects is less concentrated in SCDEW than in ΛCDM easing possible tensions with observations (e.g. Salucci et al. 2012).

By means of high resolution simulations, we then studied in detail the properties of haloes on the scales of our own Galaxy (the Milky Way) and dwarf galaxies. On MW scales, the SCDEW halo presents less substructures (30-40%) than its ΛCDM counterpart, possibly helping any "baryonic" solution (e.g. Benson et al. 2002, Macciò et al. 2010) of the so called missing satellites problem (e.g. Klypin et al. 2001). The total density profile is still well represented by an NFW fit, even though with a lower concentration parameter.

Drastic improvements on ΛCDM are however found on the scale of dwarf galaxies Thanks to the large initial thermal velocities of the warm particles (due to the very low WDM particle mass of 90 eV), the density profile in SCDEW haloes has a clear central core. The size of the core is of the order of several hundreds of parsecs, in good agreement with observations of the MW satellites like Sculptor and Fornax (e.g. Amorisco et al. 2013).

SCDEW models are still in an infant state and more simulations and theoretical work is needed to fully test them at the same level as ΛCDM . For example we have negletted the possible formation of (very small) collapsed objects in CDM before the fading of the coupling. While these objects are expected to not sensible perturb the main gravitation potential, they could still leave some signature in the observational data (e.g. secondary CMB spectrum) and ought to be included in future numerical studies.

Nevertheless our theoretical (Paper I) and Numerical (this paper) works clearly show that strongly coupled cold-warm cosmologies are able to preserve the success of ΛCDM on large scales and to *strongly* improve the agreement with data on very small scales, simultaneously easing the theoretical short-comes of DE in ΛCDM, and thus appearing as a valid alternative to a simple ΛCDM scenario.

ACKNOWLEDGMENTS

AVM and CP acknowledge support from the Sonderforschungsbereich SFB 881 "The Milky Way System" (subproject A2) of the German Research Foundation (DFG). We acknowledge the computational support from the THEO and HYDRA clusters of the Max-Planck-Institut für Astronomie at the Rechenzentrum in Garching. SAB thanks the C.I.F.S. (Consorzio Interuniversitario per la Fisica Spaziale) for its financial support.

REFERENCES

Amendola, L. 2000, Phys. Rev. D, 62, 043511
Amendola L., Tocchini-Valentini D., 2001, PhRvD, 64, 043509
Amendola L., et al., 2013, LRR, 16, 6
Amorisco N. C., Evans N. W., 2012, MNRAS, 419, 184
Amorisco N. C., Agnello A., Evans N. W., 2013, MNRAS, 429, L89
Arraki K. S., Klypin A., More S., Trujillo-Gomez S., 2014, MNRAS, 438, 1466
Avila-Reese V., Colín P., Valenzuela O., D'Onghia E., Firmani C., 2001, ApJ, 559, 516
Baldi, M., Pettorino, V., Robbers, G., & Springel, V. 2010, MNRAS, 403, 1684
Baldi, M. 2012, MNRAS, 422, 1028
Benson A. J., Frenk C. S., Lacey C. G., Baugh C. M., Cole S., 2002, MNRAS, 333, 177
Bertschinger, E., 2001, ApJS, 137, 1
Bode, P., Ostriker, J. P. & Turok, N., 2001, ApJ, 556, 93
Bonometto S. A., Sassi G., La Vacca G., 2012, JCAP, 8, 015
Bonometto S. A., Mainini R., 2014, JCAP, 3, 038
Bonometto S. A., Mainini R., Macciò A. V., 2015, MNRAS, 453, 1002
Boyarsky, A., Lesgourgues, J., Ruchayskiy, O. & Viel, M., 2009a, Journal of Cosmology and Astro-Particle Physics, 5, 12
Brax P. H., Martin J., 1999, PhLB, 468, 40
Brax P., Martin J., 2000, PhRvD, 61, 103502
Caldera-Cabral, G., Maartens, R., & Schaefer, B. M. 2009, JCAP, 7, 027
Colín, P., Valenzuela, O. & Avila-Reese, V., 2008, ApJ, 673, 203
Dalcanton, J. J. & Hogan, C. J., 2001, ApJ, 561, 35
de Blok, W. J. G., McGaugh, S. S., Bosma, A., & Rubin, V. C. 2001, ApJL, 552, L23
Di Cintio A., Brook C. B., Macciò A. V., Stinson G. S., Knebe A., Dutton A. A., Wadsley J., 2014a, MNRAS, 437, 415
Di Cintio A., Brook C. B., Dutton A. A., Macciò A. V., Stinson G. S., Knebe A., 2014b, MNRAS, 441, 2986
Dutton A. A., Courteau S., de Jong R., Carignan C. 2005, ApJ, 619, 218
Dutton A. A., Macciò A. V., 2014, MNRAS, 441, 3359
Garrison-Kimmel S., Rocha M., Boylan-Kolchin M., Bullock J. S., Lally J., 2013, MNRAS, 433, 3539

Gentile, G., Burkert, A., Salucci, P., Klein, U., & Walter, F. 2005, ApJL, 634, L145
Governato, F., Brook, C., Mayer, L., Brooks, A., Rhee, G., Wadsley, J., Jonsson, P., Willman, B., Stinson, G., Quinn, T. & Madau, P., 2010, Nature, 463, 203
Governato F., et al., 2012, MNRAS, 422, 1231
Knebe A., Devriendt J. E. G., Mahmood A., Silk J., 2002, MNRAS, 329, 813
Knollmann S. R., Knebe A., 2009, ApJS, 182, 608
Kuzio de Naray, R., McGaugh, S. S., de Blok, W. J. G., & Bosma, A. 2006, ApJS, 165, 461
Li, B., & Barrow, J. D. 2011, Phys. Rev. D, 83, 024007
Macciò, A. V., Quercellini, C., Mainini, R., Amendola, L., & Bonometto, S. A. 2004, Phys. Rev. D, 69, 123516
Macciò A. V., Dutton A. A., van den Bosch F. C., Moore B., Potter D., Stadel J., 2007, MNRAS, 378, 55
Macciò A. V., Dutton A. A., van den Bosch F. C., 2008, MNRAS, 391, 1940
Macciò, A. V., Kang, X., Fontanot, F., Sommerville, R. S., Koposov, S. E. & Monaco, P., 2010, MNRAS, 402, 1995
Macciò, A. V. & Fontanot, F., 2010, MNRAS, 404, L16
Macciò, A. V., Stinson, G., Brook, C. B., Wadsley, J., Couchman, H. M. P., Shen, S., Gibson, B. K. & Quinn, T., 2012a, ApJ, 744, L9
Macciò A. V., Paduroiu S., Anderhalden D., Schneider A., Moore B., 2012b, MNRAS, 424, 1105
Mainini R., Macciò A. V., Bonometto S. A., Klypin A., 2003, ApJ, 599, 24
Maulbetsch C., Avila-Reese V., Colín P., Gottlöber S., Khalatyan A., Steinmetz M., 2007, ApJ, 654, 53
Moore, B. 1994, Nature, 370, 629
Navarro, J. F., Frenk, C. S. & White, S. D. M., 1997, ApJ, 490, 493
Oh, S.-H., de Blok, W. J. G., Brinks, E., Walter, F., & Kennicutt, R. C., Jr. 2011, AJ, 141, 193
Oñorbe J., Boylan-Kolchin M., Bullock J. S., Hopkins P. F., Kerěs D., Faucher-Giguère C.-A., Quataert E., Murray N., 2015, arXiv, arXiv:1502.02036
Pace, F., Baldi, M., Moscardini, L., Bacon, D., & Crittenden, R. 2015, MNRAS, 447, 858
Penzo C., Macciò A. V., Casarini L., Stinson G. S., Wadsley J., 2014, MNRAS, 442, 176
Planck Collaboration, Ade, P. A. R., Aghanim, N., et al. 2014, A&A, 571, AA16
Polisensky E., Ricotti M., 2014, MNRAS, 437, 2922
Ratra B., Peebles P. J. E., 1988, PhRvD, 37, 3406
Peebles P. J., Ratra B., 2003, RvMP, 75, 559
Salucci, P., Wilkinson, M. I., Walker, M. G., et al. 2012, MNRAS, 420, 2034
Schneider A., Smith R. E., Macciò A. V., Moore B., 2012, MNRAS, 424, 684
Schneider A., Anderhalden D., Macciò A. V., Diemand J., 2014, MNRAS, 441, L6
Seljak, U., Makarov, A., McDonald, P., & Trac, H. 2006, Phys. Rev. Let., 97, 191303
Shao S., Gao L., Theuns T., Frenk C. S., 2013, MNRAS, 430, 2346
Simon J. D., Bolatto A. D., Leroy A., Blitz L., Gates E. L. 2005, ApJ, 621, 757
Springel, V., White, S. D. M., Jenkins, A., et al. 2005, Nature, 435, 629
Stadel, J., 2001, PhD Thesis, University of Washington
Strigari L. E., Frenk C. S., White S. D. M., 2014, arXiv, arXiv:1406.6079
Swaters R. A., Madore B. F., van den Bosch F. C., Balcells M., 2003, ApJ, 583, 732
Tegmark, M., & The SDSS Team. 2006, PRD, 74, 123507
Tikhonov, A. V., Gottlöber, S., Yepes, G. & Hoffman, Y., 2009, MNRAS, 399, 1611
Viel, M., Lesgourgues, J., Haehnelt, M. G., Matarrese, S., & Riotto, A., 2005, Phys. Rev. D, 71, 063534
Viel, M., Becker, G. D., Bolton, J. S., Haehnelt, M. G., Rauch, M. & Sargent, W. L. W., 2008, Physical Review Letters, 100, 041304
Viel M., Becker G. D., Bolton J. S., Haehnelt M. G., 2013, PhRvD, 88, 043502
Waler, M. G. & Peñarrubia, J. 2011, ApJ, 742, 20
Wechsler R. H., Bullock J. S., Primack J. R., Kravtsov A. V., Dekel A., 2002, ApJ, 568, 52
Wetterich C., 1988, NuPhB, 302, 668
Wetterich C., 1995, A&A, 301, 321
Zentner A. R., Bullock J. S., 2003, ApJ, 598, 49